

LETTER TO THE EDITOR

Thermal conductivity of porous aggregates

Sota Arakawa¹, Hidekazu Tanaka², Akimasa Kataoka³, and Taishi Nakamoto¹

¹ Department of Earth and Planetary Sciences, Tokyo Institute of Technology, Meguro, Tokyo, 152-8551, Japan
e-mail: arakawa.s.ac@m.titech.ac.jp

² Astronomical Institute, Tohoku University, Aoba, Sendai, 980-8578, Japan

³ Division of Theoretical Astronomy, National Astronomical Observatory of Japan, Mitaka, Tokyo, 181-8588, Japan

October 11, 2018

ABSTRACT

Context. The thermal conductivity of highly porous dust aggregates is a key parameter for many subjects in planetary science; however, it is not yet fully understood.

Aims. In this study, we investigate the thermal conductivity of fluffy dust aggregates with filling factors of less than 10^{-1} .

Methods. We determine the temperature structure and heat flux of the porous dust aggregates calculated by N -body simulations of static compression in the periodic boundary condition.

Results. We derive an empirical formula for the thermal conductivity through the solid network k_{sol} as a function of the filling factor of dust aggregates ϕ . The results reveal that k_{sol} is approximately proportional to ϕ^2 , and the thermal conductivity through the solid network is significantly lower than previously assumed. In light of these findings, we must reconsider the thermal histories of small planetary bodies.

Key words. conduction – radiative transfer – comets: general – meteorites, meteors, meteoroids

1. Introduction

Understanding the physical parameters of dust aggregates is important in planetary science. Specifically, the thermal conductivity of dust aggregates is key for determining the thermal evolution of planetary bodies, influencing the thermal evolution pathways of both rocky and icy planetesimals (e.g., Henke et al. 2012; Sirono 2017). The thermal evolution and activity of cometary nuclei also depend on the thermal conductivity of icy aggregates (e.g., Haruyama et al. 1993; Guilbert-Lepoutre & Jewitt 2011).

Dust aggregate thermal conductivity depends on many parameters, and many previous experimental studies have researched the thermal conductivity of dust aggregates with filling factors above 10^{-1} . The thermal conductivity of porous aggregates in vacuum is given by two terms: the thermal conductivity through the solid network k_{sol} and the thermal conductivity owing to radiative transfer k_{rad} . Krause et al. (2011) showed that the thermal conductivity through the solid network k_{sol} is exponentially dependent on the filling factor of dust aggregates ϕ for $0.15 < \phi < 0.54$, and concluded that the coordination number of monomer grains C influences the efficiency of heat flux within the aggregates. Sakatani et al. (2016) revealed that k_{sol} is also dependent on the contact radius between monomers r_c . The thermal conductivity owing to radiative transfer k_{rad} is affected by the temperature of dust aggregates T and the mean free path of photons l_p (e.g., Schotte 1960; Merrill 1969). Moreover, l_p depends on R and ϕ when we apply the geometrical optics approximation for the evaluation of l_p (e.g., Skorov et al. 2011; Gundlach & Blum 2012).

There are also several theoretical studies on the thermal conductivity of dust aggregates (e.g., Chan & Tien 1973; Sirono 2014; Sakatani et al. 2017). However, no previous research has

been conducted on the thermal conductivity of porous aggregates with filling factors of less than 10^{-1} , although Kataoka et al. (2013b) and Arakawa & Nakamoto (2016) revealed that the collisional growth of dust aggregates leads to planetesimal formation via highly porous aggregates with filling factors of much less than 10^{-1} . Therefore, the purpose of this study is to investigate the thermal conductivity and thermal evolution of fluffy dust aggregates in protoplanetary disks.

In this letter, we calculate thermal conductivity through the solid network k_{sol} for highly porous aggregates with filling factors in the range of 10^{-2} to 10^{-1} . We use the snapshot data of Kataoka et al. (2013a) for calculation of k_{sol} . We then validate our results through a comparison with the experimental data of Krause et al. (2011). We also derive the thermal conductivity owing to radiative transfer k_{rad} for porous aggregates of submicron-sized monomers. Our results show that the thermal conductivity of highly porous aggregates is significantly lower than previously assumed.

2. Method

2.1. Arrangement of monomer grains

The arrangement of monomer grains depends on the coagulation history of the aggregates. During initial dust aggregate coagulation in protoplanetary disks, both experimental (e.g., Wurm & Blum 1998) and theoretical (e.g., Kempf et al. 1999) studies have shown that hit-and-stick collisions lead to the formation of fractal aggregates with a fractal dimension $D \sim 2$, which is called ballistic cluster-cluster aggregation (BCCA; Meakin 1991). Furthermore, Kataoka et al. (2013a) performed three-dimensional numerical simulations of static compression of BCCA aggregates constituted from 16384 spherical grains

using a periodic boundary condition. In this study, we use snapshots of the compressed BCCA aggregates calculated by Kataoka et al. (2013a).

2.2. Temperature structure of the dust aggregate

To calculate the thermal conductivity through the solid network of an aggregate k_{sol} , we have to determine the temperature of each grain in a cubic periodic boundary. We calculate the temperature of each grain using the method of Sirono (2014). Here, we consider one-dimensional heat flow from the lower boundary plane to the upper boundary plane. There are three choices regarding the pair of lower and upper planes, and we calculate k_{sol} from three directions. Then, we average these values for each snapshot.

We define R as the monomer radius and L^3 as the volume of each cubic space. The location of the i -th grain (x_i, y_i, z_i) satisfies $|x_i| < L/2$, $|y_i| < L/2$, and $|z_i| < L/2$ for $i = 1, 2, \dots, N$, where $N = 16384$ is the number of grains in the periodic boundary. A sketch of a dust aggregate in a cubic periodic boundary is shown in Fig. 1. Here, we assume that heat flow occurs along the z -direction. The grains located in $-L/2 < z_i < -(L/2 - R)$ are on the lower boundary (#1 in Fig. 1), and the grains located in $+(L/2 - R) < z_i < +L/2$ are on the upper boundary (#40 in Fig. 1). If the i -th grain is located on the lower (upper) boundary, we add a new grain on the upper (lower) boundary. The location of the new grain is $(x_i, y_i, z_i + L)$ if the i -th grain is located on the lower boundary (#X in Fig. 1) and $(x_i, y_i, z_i - L)$ if the i -th grain is located on the upper boundary (#Y in Fig. 1). We set the temperature of grains located on the lower (#1 and #Y in Fig 1) and upper (#40 and #X in Fig 1) boundary as $T_0 + \Delta T/2$ and $T_0 - \Delta T/2$, respectively.

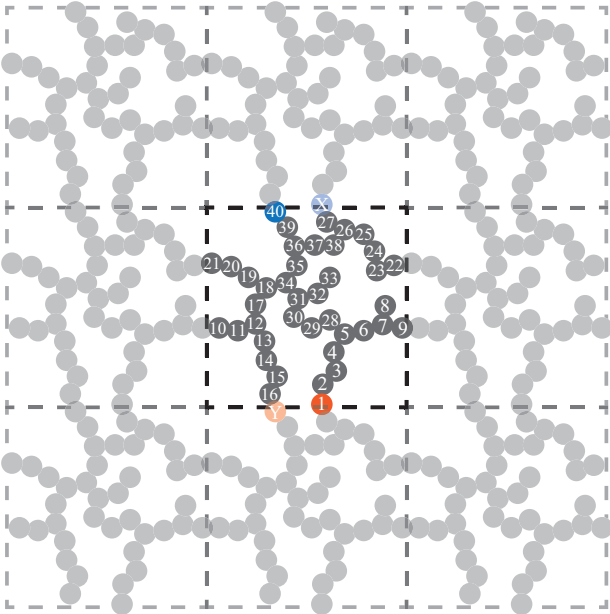


Fig. 1. Sketch of a dust aggregate in a cubic periodic boundary. The temperature of grains located on the lower (#1 and #Y) and upper (#40 and #X) boundary is set to $T_0 + \Delta T/2$ and $T_0 - \Delta T/2$, respectively. The temperature of each grain is calculated by solving Eq. (1) simultaneously for each grain.

Heat flows through the monomer-monomer contacts, and for steady state conditions, the equation of heat balance at the i -th

grain is given by

$$\sum_j F_{i,j} = 0, \quad (1)$$

where $F_{i,j}$ is the heat flow from the j -th grain to the i -th grain, given by

$$F_{i,j} = H_c(T_j - T_i), \quad (2)$$

where H_c is the heat conductance at the contact of two grains, and T_i and T_j are the temperatures of the i -th and j -th grains, respectively. We consider the contacts not only inside the periodic boundary but also on the side boundaries (e.g., the contacts between #9 and #10 and between #21 and #22 in Fig. 1). The heat conductance at the contact of two grains H_c is (Cooper et al. 1969)

$$H_c = 2k_{\text{mat}}r_c, \quad (3)$$

where k_{mat} is the material thermal conductivity and r_c is the contact radius of monomer grains. The contact radius r_c depends on the monomer radius R and the material parameters (Johnson et al. 1971). The heat conductance within a grain H_g is also given by (Sakatani et al. 2017)

$$H_g = \left(\frac{4\pi}{3}\right)^{1/3} k_{\text{mat}}R. \quad (4)$$

However, we neglect the effect of H_g because H_g is sufficiently larger than H_c for (sub)micron-sized grains. Therefore, the temperature structure of the aggregate in the cubic periodic boundary can be calculated by solving Eq. (1) simultaneously for all N grains except lower and upper boundary grains.

2.3. Thermal conductivity through the solid network

Once the temperature structure is obtained, we can calculate the total heat flow at the upper boundary $\sum_{\text{upper}} F_{i,j}$, where we take the sum of contacts between the upper boundary i -th grain and internal j -th grain (for the case of Fig. 1, $\sum_{\text{upper}} F_{i,j} = F_{X,27} + F_{40,39}$). The total heat flow at the upper boundary $\sum_{\text{upper}} F_{i,j}$ can be rewritten using the thermal conductivity through the solid network k_{sol} as

$$\sum_{\text{upper}} F_{i,j} = k_{\text{sol}} \frac{\Delta T}{L} L^2. \quad (5)$$

In this study, we discuss k_{sol} as a function of the filling factor ϕ , and rewrite L using ϕ as

$$L = \left(\frac{4\pi N}{3\phi}\right)^{1/3} R. \quad (6)$$

Therefore, we obtain k_{sol} as a function of ϕ as follows:

$$\begin{aligned} k_{\text{sol}} &= \frac{1}{L\Delta T} \sum_{\text{upper}} F_{i,j}, \\ &= 2k_{\text{mat}} \frac{r_c}{R} \cdot \left(\frac{3\phi}{4\pi N}\right)^{1/3} \sum_{\text{upper}} \frac{T_j - T_i}{\Delta T}, \\ &\equiv 2k_{\text{mat}} \frac{r_c}{R} \cdot f(\phi), \end{aligned} \quad (7)$$

where $f(\phi)$ is a dimensionless function of ϕ . Note that the total heat flow at the lower boundary $-\sum_{\text{lower}} F_{i,j}$ is clearly equal to $\sum_{\text{upper}} F_{i,j}$ considering the heat balance.

3. Results

Here, we present the dimensionless function $f(\phi)$ for nine snapshots from three runs and three densities (Table 1). We calculated $f(\phi)$ in three directions for each snapshot and took the arithmetic mean values. Note that the compressed BCCA aggregates might be isotropic if the number of monomer grains is sufficiently large; thus, we only discuss the mean values of $f(\phi)$.

Table 1. Numerical calculation results.

run	ϕ	$f(\phi)$
□	1.01×10^{-2}	1.44×10^{-4}
□	3.02×10^{-2}	1.12×10^{-3}
□	9.91×10^{-2}	1.04×10^{-2}
△	1.00×10^{-2}	3.86×10^{-5}
△	3.00×10^{-2}	5.24×10^{-4}
△	1.00×10^{-1}	6.24×10^{-3}
○	9.98×10^{-3}	4.14×10^{-5}
○	2.99×10^{-2}	5.15×10^{-4}
○	9.99×10^{-2}	9.05×10^{-3}

Figure 2 shows the dimensionless function $f(\phi)$ as a function of the filling factor ϕ . The best-fit line given by the least-squares method (green dashed line) is

$$f(\phi) = 1.18\phi^{2.14}. \quad (8)$$

Hereafter, we utilize the following more simple relationship between $f(\phi)$ and ϕ (magenta solid line)

$$f(\phi) = \phi^2. \quad (9)$$

Sakatani et al. (2017) predicted that $f(\phi) = (2/\pi^2)C\phi$, where C is the coordination number. For highly porous aggregates, the coordination number C is approximately two, and the filling factor dependence on C is weak. Hence, $f(\phi)$ would be proportional to ϕ in the model of Sakatani et al. (2017); however, in reality, $f(\phi)$ is approximately proportional to ϕ^2 .

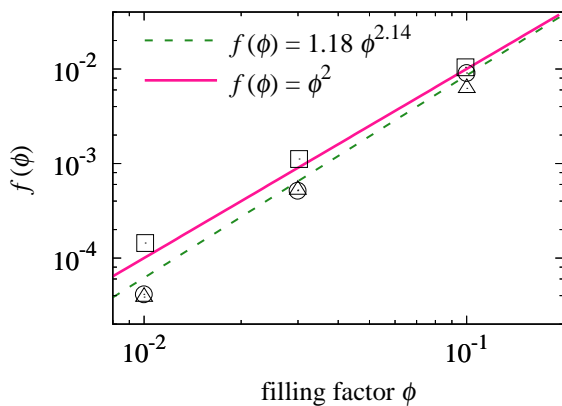


Fig. 2. Fitting of the dimensionless function of thermal conductivity $f(\phi)$ as a function of the filling factor ϕ . The green dashed line is the best-fit line and the magenta solid line represents the simple function $f(\phi) = \phi^2$.

In the context of the thermal conductivity of colloidal nanofluid and nanocomposites, Evans et al. (2008) revealed that thermal conductivity is strongly affected by the fraction of linear chains that contribute to heat flow in the aggregates. The contributing grains are called backbone grains, and non-contributing

grains are called dead-end grains (#8, #32, and #33 in Fig. 1; Shih et al. 1990). We will discuss the effects of different fractions of backbone and dead-end grains on the thermal conductivity in future research.

By comparing our model to the experimental data of Krause et al. (2011), we can confirm the validity of our model (Fig. 3). The magenta line in Fig. 3 represents the calculated thermal conductivity from Eqs. (7) and (9), the blue curve is the exponential fitting of experimental data, $k_{\text{sol}} = 1.4e^{7.91(\phi-1)} \text{ W m}^{-1} \text{ K}^{-1}$ (Krause et al. 2011), and the black dashed line is a model commonly used to study the thermal evolution of planetary bodies, that is, $k_{\text{sol}} = \phi k_{\text{mat}}$ (e.g., Sirono 2017). Both experimental (crosses) and numerical (squares, triangles, and circles) data are plotted.

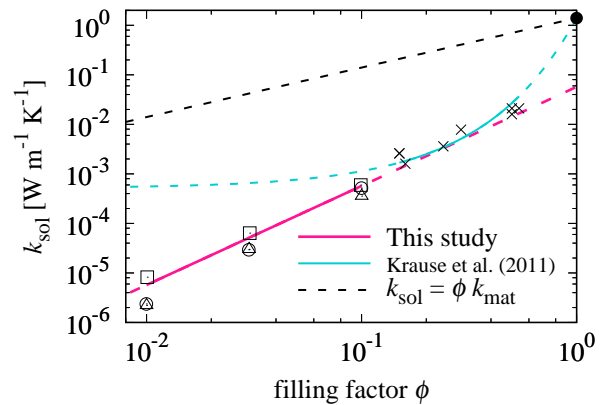


Fig. 3. Experimental (crosses) and numerical (squares, triangles, and circles) data of thermal conductivity through the solid network k_{sol} . Our model (magenta line) was compared to the experimental fitting data of Krause et al. (2011, blue curve).

When we consider the dust aggregates of (sub)micron-sized monomers, the contact radius between monomers r_c is given by (Johnson et al. 1971)

$$r_c = \left(\frac{9\pi\gamma(1-\nu^2)}{2YR} \right)^{1/3} R, \quad (10)$$

where $\gamma = 25 \text{ mJ m}^{-2}$, $\nu = 0.17$, and $Y = 54 \text{ GPa}$ are the surface energy, Poisson's ratio, and Young's modulus of SiO_2 grains, respectively (Wada et al. 2007). We set $R = 0.75 \text{ }\mu\text{m}$ and $k_{\text{mat}} = 1.4 \text{ W m}^{-1} \text{ K}^{-1}$ to the same values as Krause et al. (2011). Figure 3 clearly shows that our empirical model is applicable to the k_{sol} of porous aggregates with filling factors of $\phi \sim 0.1$. Moreover, our model is applicable not only for $\phi \lesssim 0.1$ but also for the range $0.1 \lesssim \phi \lesssim 0.5$.

Note that most of the experimental data of k_{sol} are fitted using exponential functions of ϕ , which pass the material thermal conductivities (e.g., Krause et al. 2011; Henke et al. 2013). However, when we consider the thermal conductivity through the solid network, i.e., thermal conductivity limited by the necks between two monomers, k_{sol} must be given by $k_{\text{sol}} \sim (r_c/R)k_{\text{mat}}$, even for dense dust aggregates whose filling factors are close to unity (e.g., Chan & Tien 1973).

4. Discussion

Finally, we evaluate the total thermal conductivity of porous icy aggregates under vacuum conditions. Thermal conductivity

through the solid network k_{sol} is given by

$$k_{\text{sol}} = 2k_{\text{mat}} \frac{r_c}{R} \phi^2, \quad (11)$$

and thermal conductivity owing to radiative transfer k_{rad} is given by (Merrill 1969)

$$k_{\text{rad}} = \frac{16}{3} \sigma_{\text{SB}} T^3 l_p, \quad (12)$$

where $\sigma_{\text{SB}} = 5.67 \times 10^{-8} \text{ W m}^{-2} \text{ K}^{-4}$ is the Stefan-Boltzmann constant. We calculate the mean free path of photons in fluffy aggregates of submicron-sized grains l_p as follows:

$$l_p = \frac{1}{(\kappa_{\text{abs}} + \kappa_{\text{sca}}) \rho_{\text{mat}} \phi}, \quad (13)$$

where κ_{abs} and κ_{sca} are the absorption and scattering mass opacities of monomers, respectively, and $\rho_{\text{mat}} = 1.68 \times 10^3 \text{ kg m}^{-3}$ is the material density. Here, the composition of icy dust aggregates is consistent with Pollack et al. (1994). The total mass opacity of submicron-sized monomers $\kappa_{\text{abs}} + \kappa_{\text{sca}}$ is hardly dependent on the wavelength of the thermal radiation $\lambda = 2.9 \times 10^{-3} (T/\text{K})^{-1} \text{ m}$ for $10^{-6} \text{ m} < \lambda < 10^{-4} \text{ m}$, and $\kappa_{\text{abs}} + \kappa_{\text{sca}}$ is on the order of $10^2 \text{ m}^2 \text{ kg}^{-1}$ (e.g., Kataoka et al. 2014). Then we set $l_p = 10^{-5} \phi^{-1} \text{ m}$ in this study. Note that, for the case of fluffy aggregates of submicron-sized monomers, the wavelength λ is larger than the monomer radius R , even if the temperature is on the order of 10^3 K . Hence, we cannot apply the geometrical optics approximation for the evaluation of l_p .

Figure 4 shows the k_{sol} of crystalline and amorphous icy aggregates, $k_{\text{sol,cr}}$ and $k_{\text{sol,am}}$, and the thermal conductivity owing to radiative transfer k_{rad} for aggregates composed of icy monomers with a radius of $R = 0.1 \mu\text{m}$ and temperature of $T = 40 \text{ K}$. We set $\gamma = 100 \text{ mJ m}^{-2}$, $\nu = 0.25$, and $Y = 7 \text{ GPa}$ for icy grains (Wada et al. 2007). The material thermal conductivities of crystalline and amorphous grains, $k_{\text{mat,cr}}$ and $k_{\text{mat,am}}$, are given by $k_{\text{mat,cr}} = 5.67 \times 10^2 (T/\text{K})^{-1} \text{ W m}^{-1} \text{ K}^{-1}$ and $k_{\text{mat,am}} = 7.1 \times 10^{-8} (T/\text{K}) \text{ W m}^{-1} \text{ K}^{-1}$, respectively (Haruyama et al. 1993).

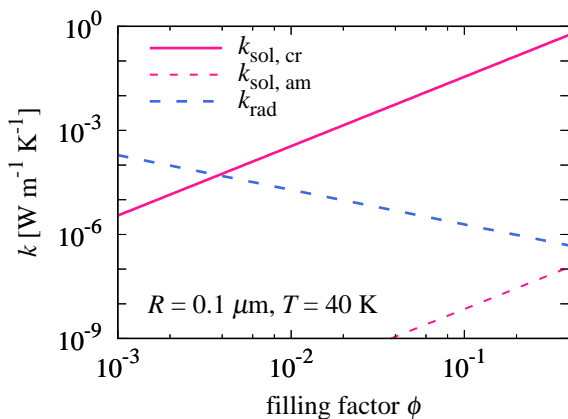


Fig. 4. Comparison between k_{sol} (magenta solid line for crystalline icy aggregates and magenta dashed line for amorphous) and k_{rad} (blue dashed line). The monomer radius is $R = 0.1 \mu\text{m}$ and the temperature is $T = 40 \text{ K}$.

For the case of $\phi < 4 \times 10^{-3}$, the thermal conductivity owing to radiative transfer k_{rad} is larger than the thermal conductivity through the solid network of crystalline icy aggregates $k_{\text{sol,cr}}$, even if the temperature is sufficiently low ($T = 40 \text{ K}$).

If the total thermal conductivity $k_{\text{sol}} + k_{\text{rad}}$ does not change substantially when crystallization occurs, then the internal temperature of icy planetesimals could still increase after crystallization, which might cause runaway crystallization due to latent heat. In addition, when the temperature of an icy planetesimal increases, sintering can proceed inside the icy aggregate before monomer grains evaporate or melt (e.g., Sirono 2017). We cannot evaluate the contact radius r_c from Eq. (10) when aggregates are sintered, and k_{sol} increases linearly as a consequence of the increase of r_c . Sintering might also affect the mechanical strength of aggregates (e.g., Omura & Nakamura 2017) and the critical velocity for collisional growth (e.g., Sirono & Ueno 2017). Therefore, the growth pathways of icy planetesimals might be altered by sintering of icy aggregates. Not only icy planetesimals but also rocky aggregates could experience sintering before growing into dm-sized bodies, which might explain the retention of chondrules inside fluffy aggregates (Arakawa 2017). Note also that the total thermal conductivity might be controlled by the thermal conductivity due to gas diffusion for the case of fluffy aggregates in high gas density environments (e.g., the innermost region of protoplanetary disks and/or planetary surfaces; Piqueux & Christensen 2009).

In conclusion, we have revealed the filling factor dependence of the thermal conductivity of porous aggregates. We showed that the thermal conductivity of highly porous aggregates is significantly lower than previously assumed. In future work, we will reexamine the growth pathways of planetesimals in protoplanetary disks, and combine this with a density and thermal evolution analysis.

Acknowledgements. We thank the referee Gerhard Wurm for constructive comments. This work is supported by JSPS KAKENHI Grant (15K05266). S.A. is supported by the Grant-in-Aid for JSPS Research Fellow (17J06861).

References

- Arakawa, S. 2017, *ApJ*, 846, 118
Arakawa, S. & Nakamoto, T. 2016, *ApJ*, 832, L19
Chan, C. K. & Tien, C. L. 1973, *Journal of Heat Transfer*, 95, 302
Cooper, M. G., Mikic, B. B., & Yovanovich, M. M. 1969, *International Journal of Heat and Mass Transfer*, 12, 279
Evans, W., Prasher, R., Fish, J., et al. 2008, *International Journal of Heat and Mass Transfer*, 51, 1431
Guilbert-Lepoutre, A. & Jewitt, D. 2011, *ApJ*, 743, 31
Gundlach, B. & Blum, J. 2012, *Icarus*, 219, 618
Haruyama, J., Yamamoto, T., Mizutani, H., & Greenberg, J. M. 1993, *J. Geophys. Res.*, 98, 15
Henke, S., Gail, H.-P., Trieloff, M., & Schwarz, W. H. 2013, *Icarus*, 226, 212
Henke, S., Gail, H.-P., Trieloff, M., Schwarz, W. H., & Kleine, T. 2012, *A&A*, 537, A45
Johnson, K. L., Kendall, K., & Roberts, A. D. 1971, *Proceedings of the Royal Society of London Series A*, 324, 301
Kataoka, A., Okuzumi, S., Tanaka, H., & Nomura, H. 2014, *A&A*, 568, A42
Kataoka, A., Tanaka, H., Okuzumi, S., & Wada, K. 2013a, *A&A*, 554, A4
Kataoka, A., Tanaka, H., Okuzumi, S., & Wada, K. 2013b, *A&A*, 557, L4
Kempf, S., Pflanzner, S., & Henning, T. K. 1999, *Icarus*, 141, 388
Krause, M., Blum, J., Skorov, Y. V., & Trieloff, M. 2011, *Icarus*, 214, 286
Meakin, P. 1991, *Reviews of Geophysics*, 29, 317
Merrill, R. B., 1969, *Nasa Technical Note*, D-5063
Omura, T. & Nakamura, A. M. 2017, *Planet. Space Sci.*, in press [arXiv:1708.08038]
Piqueux, S. & Christensen, P. R. 2009, *J. Geophys. Res.*, 114, E09005
Pollack, J. B., Hollenbach, D., Beckwith, S., et al. 1994, *ApJ*, 421, 615
Sakatani, N., Ogawa, K., Iijima, Y.-i., et al. 2017, *AIP Advances*, 7, 015310
Sakatani, N., Ogawa, K., Iijima, Y.-i., Arakawa, M., & Tanaka, S. 2016, *Icarus*, 267, 1
Schotte, W. 1960, *AIChE Journal*, 6, 63
Shih, W.-H., Shih, W. Y., Kim, S.-I., Liu, J., & Aksay, I. A. 1990, *Phys. Rev. A*, 42, 4772
Sirono, S.-i. 2014, *Meteoritics and Planetary Science*, 49, 109
Sirono, S.-i. 2017, *ApJ*, 842, 11
Sirono, S.-i. & Ueno, H. 2017, *ApJ*, 841, 36
Skorov, Y. V., van Lieshout, R., Blum, J., & Keller, H. U. 2011, *Icarus*, 212, 867
Wada, K., Tanaka, H., Suyama, T., Kimura, H., & Yamamoto, T. 2007, *ApJ*, 661, 320
Wurm, G. & Blum, J. 1998, *Icarus*, 132, 125